Understanding regional mechanics of rat myocardia by fitting hyperelatsic models

Fulufhelo Nemavhola (masitfj@unisa.ac.za)
University of South Africa
Harry Ngwangwa
University of South Africa
Thanyani Pandelani
Council for Scientific and Industrial Research (CSIR)
Neil Davies
University of Cape Town
Thomas Franz
University of Southampton

Research Article

Keywords: Cardiac mechanics, experimental mechanics, sheep heart mechanics, hyperelatic constitutive model fitting, soft tissue mechanics, biaxial testing

Posted Date: October 25th, 2021

DOI: https://doi.org/10.21203/rs.3.rs-957393/v1

Understanding regional mechanics of rat myocardia by fitting hyperelatsic constitutive models

Fulufhelo Nemavhola[a*], Harry Ngwangwa[a], Thanyani Pandelani[a,b] Neil Davies[d], Thomas Franz[e,d,f,g]

[a]*Unisa Biomedical Engineering Research Group, Department of Mechanical Engineering, School of Engineering, College of Science Engineering and Technology, University of South Africa, Pretoria, 0001, South Africa,*
[b]*Defence and security, Council for Scientific and Industrial Research (CSIR), Pretoria, 0001, South Africa*
[d]*Division of Biomedical Engineering, Department of Human Biology, University of Cape Town, Observatory 7925, South Africa*
[e]*Cardiovascular Research Unit, Department of Surgery, University of Cape Town, Observatory 7925, South Africa*
[f]*Centre for High Performance Computing, Rosebank 7700, South Africa*
[g]*Bioengineering Science Research Group, Engineering Sciences, Faculty of Engineering and the Environment, University of Southampton, Southampton SO171BJ, UK*
* *Correspondence: masitfj@unisa.ac.za ; Tel.: (+27 (011) 471 2765)*

Abstract

Availability of biaxial mechanical data for heart myocardia remains high in demand for the development of accurate and detailed computational models. The aim of this study is to study the regional difference of wall mechanics using rat heart in the left ventricle (LV), septal wall (STW) and right ventricle (RV). This was achieved by conducting a biaxial test on three rat heart myocardia (i.e LV, RV and STW). Fung, Choi-Vito, Polynomial (Anistropic), Four-Fiber family, Holzapfel (2000) and Holzapfel (2005) hyperelastic models were selected and fitted on the bixial data of the LV, RV and STW. The best hyperelastic model was the selected based on evaluation index (EI) determined from the coefficient of determination (R^2). All the six models were then compared in all three rat heart myocardia. The results show that the Polynomial (Anisotropic) model outperforms the other five models in all myocardial tissues with EI's above 90 % goodness of fit. The Four-fiber-family and the two Holzapfel models perform equally in the LV and STW myocardial tissue between 50 and 70 % goodness of fit. The Fung and Choi-Vito models yielded poor goodness of fit in the LV and STW myocardial tissues. Parameter fitting is useful method in advancing reliable data to be used in the development of accurate computational models.

Keywords: *Cardiac mechanics, experimental mechanics, sheep heart mechanics, hyperelatic constitutive model fitting, soft tissue mechanics, biaxial testing*

1. Introduction

Studying of cardiac wall mechanics is vital in understanding heart failure and also for the development of reliable and accurate heart computational models for predicting cardiac wall performances. Computational models are vital in the understanding of regional and global function of the heart after medical intervention. Cardiovascular diseases are regarded to be the leading cause of death globally. Heart failure that normally leads to cardia arrest may be due to heart disease such as myocardial infarction and myocardial ischemia. The important function of the heart that have ben placed on LV has resulted in over concentration of LV mechanics. For example, for some time, it was reported that mechanisms and importance of RV only started to happen in the late 1950s [1]. Over concentration on LV mechanics has resulted in the over-reliance of LV mechanics data in the development of computational models. This problem has to a certain extend compromised the accuracy of heart computational model because it is now begun to be understood that the cardiac mechanics of left ventricle, septal wall and right ventricle may be different. Therefore, an in-depth study of the mechanics of all heart walls including left ventricle, septal wall and right ventricle is vital to improve the accuracy of heart models during development.

Generally, study of mechanical behaviour of soft tissues has sparked interest as this has the ability to provide insight on how diseases progresses [2-5]. Previous pig heart was used to study the various of mechanical properties across regions [4, 5]. Given the large deformation of heart cardiac wall, most researchers are using computational models like Finite Element Models to study mechanisms of various heart diseases including myocardial infarction and myocardial ischemia. Hence, understanding the mechanical properties of heart myocardia is critical for both basic and clinical

researchers. Numeral analysis has been previous utilised in understanding the global and regional functioning of the heart [6-14]. Previously, Finite Element analysis was utilised to study the effect of myocardial infarction using the 3D subject specific model of the rat heart [12-14].

Computational models of heart have shown progress towards understanding of how diseases progress. However, the assumption that LV exhibits the same mechanical properties as RV and STW may be inaccurate. Most developed computational models have assumed that the mechanical properties of the whole 3D heart models [15] were the same. Even though the biomechanical analysis of the LV has provided some light in the area of computational analysis of the heart [16], there is a need to ascertain the mechanical differences between LV, STW and RV.

Algorithms have been globally utilised to determine the material properties of various biological tissues. Material parameters of healthy myocardium have been determined from mainly one region, that is, the left ventricle (LV). The work presented here shows the biaxial data in three main regions of the rat heart, namely, LV, RV and STW. The mechanical properties of LV, RV and STW regions were mechanically characterised using the biaxial test. Most studies focus on the mechanical characterisation of LV subjected to various conditions. Therefore, there is a need to determine the passive mechanical material parameters of an anisotropic constitutive model for myocardial infarcts in rats. In this study, the mean biaxial stress-strain data in three regions in the rat heart (i.e RV, LV and STW) was utilised in determining the material properties of the Fung [17], Choi-Vito model [18], Holzapfel (2000) [19], Holzapfel (2005)[20], Four-fiber family model[21, 22], and the Polynomial (Anisotropy) model[23]. The passive

material parameters of the various regions in the rat heart were obtained by utilising the algorithm was error between the experimental and predicted data is minimised.

The objective of this study was to investigate the regional difference of cardiac mechanics in healthy rat heart by fitting six hyperelastic models. Most studies have been focusing on studying the mechanical properties of single heart chamber, especially the left ventricle free wall. In some instances, there has been attempted to study the biomechanical properties of right ventricle free wall [24-28] but to our knowledge limited studies have focussed on the septal wall. The hypothesis is that heart walls (i.e left ventricle, septal wall, and right ventricle) may not exhibit the same mechanical properties. To verify this hypothesis, the experimental data was obtained by subjecting heart myocardium to biaxial testing. The force and displacement data were then converted into stress and strain for curve fitting of different hyperelastic models. The difference between wall mechanics in various region of the rat heart was shown and studied to show how cardiac wall mechanics may differ significantly across rat heart regions.

2. Anisotropic hyperelastic modeling

There are typically two different approaches that have been used for representation of anisotropy in soft tissues: first one is based on the use of Green-Lagrange components [17, 18, 19] and the second one is based on the use of strain invariants. The Green-Lagrange components based approaches involve expressing the strain energy density functions W as summations of different contributions of the Green-Lagrange strain tensor E_{ij}. Ateshian and Costa [29][20] state that this formulation allows the uncoupling of the strain energy function into dilatational and distortional parts which

facilitates the computational implementation of incompressibility. However, it is reported by Chagnon et al [30] that these constitutive models have many material properties which may make cause convergence issues as well as numerical instabilities. The other difficulty with these models is that they have no physical significance, hence makes them very hard to fit.

The strain invariant-based approach expresses the strain energy density function W based on combinations of different isotropic and anisotropic functions. The isotropic and anisotropic functions are given as strain invariants, I_k. There are three different implementations of this in the literature comprising polynomial, power and exponential implementations, with the latter being the most popular because it includes the strain hardening effect in soft tissue. There are other forms of the strain invariant-based methods in the literature that implement logarithmic or tangent functions. However, these forms are specifically suitable for the modelling of moderate deformation especially before soft tissue activation.

In this paper, six anisotropic hyperelastic models are used to study the variances in the three walls of the rat heart. The six models are: the Fung [17] , Choi-Vito model [18], Holzapfel (2000) [19], Holzapfel (2005) [20], Four-fiber family model [21, 22], and the polynomial anisotropy model [23]. To understand the different performances of these models it is important to highlight their strain energy density function representations. The strain energy density functions for the models are presented in Table.

In *Table* 1, the Fung and Choi-Vito material models are both based on the Green-Lagrange component method with different implementations. The other four material models are based on strain invariants with the two Holzapfel models being strongly

exponential in form. The four-fiber family material model is a hybrid of polynomial and exponential form of implementation. A significant characteristic of the strain invariant approaches is the inclusion of the anisotropic function of strain invariants I_4 and/or I_6 in their strain energy density functions.

3. Experimental methods

3.1 Heart dissection and testing sample preparation

The methodology presented in this study was first reported in our previous articles [31, 32]. Rats (Wistar) of the weight between 200 and 250 grams were sacrificed humanely inhaling 5 % of halothane at the University of Cape Town, Cape Town. The heart was taken out of the animal only after the heartbeat and breathing had completely stopped. After this process, the rat hearts were delivered to the Unisa Biomechanics Lab University of South Africa, Johannesburg for further processing and testing. The samples were put in a temperature regulated box to ensure maintenance of temperature between 0 ^{o}C to 6 ^{o}C. To be consistent in performing the biaxial testing, the outflow (OT) direction was targeted as the main direction and 90o to the OT was measured and regarded the circumferential direction. The 9x9 mm samples were dissected from the LV, RV and STW. Within 2 hours of arrival, the mechanical testing was performed on the prepared samples. The animal study ethics was approved by the Faculty of Health Sciences Animal Ethics Committee of the University of Cape Town on 6 May 2019 under reference number FHS AEC REF 019-019 [31].

3.2 Biaxial tensile test

The mechanical properties of the rat myocardia in the LV, RV and STW regions was performed by utilising the customed biaxial tensile material apparatus (BioTester 5000 CellScale, Waterloo, Canada) [33, 34]. The clamps of BioRake design was used for piercing the tissue samples, see Figure 1. A 5x5 mm of the sample size was clamped on the biaxial BioRake allowing the overlap of approximately 2.5 mm as shown in Figure 2, the rat myocardia were clamped and subjected to eqi-biaxial testing. Vernier calliper weas utilised in measuring the thickness of the samples. This measurement was done carefully in trying to minimise the error to poor or inaccurate thickness measurement. To reduce these errors, four to five measurement were taken from each sample and the average thickness was then used for further process of the results. The precondition was performed before testing and collecting dtat by subjecting each sample to a 10 % strain at a rate of 0.08 per seconds. During testing 0.005 N of force was applied for 0.53 seconds as a preload. Also, all samples were preconditioned by applying 40 N/m of eqi-biaxial tension as previously described [16]. The body temperature was mimicked by immersing all harvested samples in the saline 0.91 % w/v of NaCl solution and heated and maintained at 37 ^{o}C. in collecting the biaxial testing data, in each sample, 40 % of strain was applied in both the longitudinal and circumferential direction at the strain rate of 0.08 per seconds. Most studies have reported between 25 % [16], 35 % [35] and 60 % [36] of strain in the rat heart however this study 40 % strain was then selected.

3.3 Numerical analysis

A Powell method implemented as 3rd Party library algorithm in HYPERFIT software (v8.1.0.604) was used to fit the Fung, Choi-Vito, Polynomial (anisotropic), Holzapfel (2000), Holzapfel (2005) and Four-Fibre-Family strain energy functions to the biaxial experimental data, as shown in Table 1. All curves were then averaged to obtained the material parameters

of each hyperelastic model from the average strees vs strain curves [37]. Therefore, to obtain average curves of each specimen, engineering stresses and strains data was obtained using the same frequency and stresses and strains were calculated using Eqs. (1) and (3).

The recorded force and displacement from both longitudinal and circumferential directions were converted to the engineering stress and strain, respectively.

$$\sigma_{c,l} = \frac{F_{c,l}}{A_{c,l}} \qquad (1)$$

Where $A_{c,l}$ is the cross-sectional area in the circumferential and longitudinal direction and calculated as follows:

$$A_{c,l} = l_{c,l} x b_{c,l} \qquad (2)$$

The engineering strain is calculated as follows:

$$\varepsilon_{c,l} = \frac{l_o - l_i}{l_0} \qquad (3)$$

In Figure 3, the areas between the loading and unloading curves show the amount of energy that is dissipated due to internal material friction in both directions. This is attributed to the viscoelastic property of the cardiac tissue. However, the amount of dissipated energy in the cardiac tissue seems to be much higher that exhibited by other connective soft tissue such as tendons. This implies that cardiac tissue does not really return all the absorbed tension energy on contraction. The amount of dissipated energy is greater for the left ventricle and mid-wall myocardial tissues than it is for the right ventricle tissues. Furthermore, the dissipated energy is greater in the longitudinal direction than in the circumferential direction.

4 Results

Though studies have shown that RV and LV are embryologically [38] structurally [39, 40] and functionally [41] distinct, there are a number of technical aspects related to the underlying structural differences that remain unclear. In this study, the coefficients of determination or correlation coefficients (R^2) for each of the six constitutive models are plotted in Figure 4 on fourteen test samples. The metric R^2 measures how much variability in the dependent variable can be explained by the model. It is calculated by

$$R^2 = 1 - \frac{\sum_i (y_i - \hat{y}_i)^2}{\sum_i (y_i - \bar{y})^2} \quad (1)$$

Where the index i represents a particular data point, y is the real value, $\hat{y}$ is the predicted value and $\bar{y}$ is the mean of the real values. This is a good measure of how well the model fits the dependent variable. However, it should be noted that the R^2 does not consider the overfitting problem.

The three R^2 plots in Figure 3 present results from (a) the left ventricle – LV (b) the mid-wall – STW and (c) the right ventricle – RV walls. The polynomial model yields consistently higher correlation coefficients over all myocardial tissues and on almost every test at above 90%. On the other hand, the Fung model yields lowest correlation coefficients at around 70%. Among the three tissues, the models predict myocardial tissue behaviour of LV and STW much better than that of the RV tissue. The correlation coefficients for the best performing models are around above 95% for LV and STW while that for the RV tissue are around 90%. The performances of the polynomial, four-fiber-family, and the Holzapfel (both 2000 and 2005 versions) models closely match each other for the LV and STW tissues. This is not exactly the case for the RV myocardial tissue which is a further confirmation of how the LV differs from the RV myocardium. Some studies have attributed these differences to the differences in the arrangement and distribution of the sarcomere lengths within the two ventricles [21]. The differences seem to be adapted to their different functionalities in that the LV serve the systematic circulation of blood to the entire body while the RV serve the pulmonary circulation which exhibits low resistance and high compliance in order to maintain mean and pulse

pressure which is typically lower than the systematic circulation [42]. Sacks and Chuong [43] have further reported that the longitudinal direction stiffness were greater in the RV than in the LV and that the degree of anisotropy was greater in the RV than in the LV. These findings were also supported in our previous experimental investigations in which cross-directional and cross-wall differences were studied [20]. These differences require more investigation into the structure and composition of the RV myocardial tissue. The results reported here are a further demonstration of how the RV myocardial tissue seems to possess its own mechanical characteristics that are distinct from those of the LV and STW tissue.

The coefficients of determination or correlation coefficients (R^2) for each of the six constitutive models are plotted in Figure 4 on fourteen test samples. The three plots represent results from (a) the left ventricle – LV (b) the mid-wall – STW and (c) the right ventricle walls. The polynomial model yields consistently higher correlation coefficients over all myocardial tissues and on almost every test at above 90 %. On the other hand, the Fung model yields lowest correlation coefficients at around 70 %. Among the three tissues, the models predict myocardial tissue behaviour of LV and STW much better than that of the RV tissue. The correlation coefficients for the best performing models are around above 95 % for LV and STW while that for the RV tissue are around 90 %. The performances of the polynomial, four-fiber-family, and the Holzapfel (both 2000 and 2005 versions) models closely match each other for the LV and STW tissues. This is not exactly the case for the RV myocardial tissue. These differences require more investigation into the structure and composition of the RV myocardial tissue. These results are a further demonstration of how the RV myocardial tissue seems to possess its own mechanical characteristics that are distinct from those of the LV and STW tissue.

Similar trends as the correlation coefficients were observed in the Evaluation Indices (EI's) plotted in Figure 4. Notice that the EI's are exactly similar for LV and STW tissues while the RV tissues yield different EI's. In Figure 7, only the Fung and Choi-Vito models show huge

variations in the fitting performances for the on the LV and STW myocardial tissues. For the RV myocardial tissue, all models show substantial amounts of variations across.

In this study, the differences were investigated by observing the differences in the six different models and their prediction capabilities. This was carried out by examining what model parameters make the polynomial model outperform the other five models; what are the common features between the LV and STW myocardial tissues that make the polynomial, four-fiber-family, and the two Holzapfel models approximate their behaviour better than the other models; and what unique parameters are there in the polynomial model that enables it to model RV tissue behaviour the best.

A closer examination of the parameters of the six models shows that the polynomial, four-fiber-family and two Holzapfel models share one feature in that they all account for fiber orientations. It would therefore imply that to some extent this common feature contributes towards their superiority when modelling LV and STW tissue behaviour. The Fung and Choi-Vitto models do not seem to have this in their architecture. This may be the cause of their huge variability in the modelling of the LV and STW as compared to the other models in Figure 7.

In addition to the above observation, the polynomial and four-fiber-family model incorporate effects of anisotropy. It is observed that these two models have cross-directional material parameters in their architectures. The implementations of the anisotropy in the two models are different. Though the differences do not yield much significantly different results for the LV and STW myocardia, the differences are significant for the RV myocardial tissues. It is also important to note that the polynomial model has four more material parameters than the four-fiber-family model. This might imply that the degree of anisotropy in the RV might be much more complex than that in the LV and STW tissues. Hence the prediction of its mechanical behaviour can be best achieved by models that sufficiently incorporate anisotropy besides Fiber orientation.

However, it is equally important to discuss the computational efficiencies of the models under investigation. In this study it is remarkable how a five-parameter Holzapfel (2005) model closely matched an eight-parameter Four-Fiber-family and a twelve-parameter polynomial models in predicting the behaviour of the LV and STW tissues. In terms of computational efficiency, this model clearly outperforms the other two big-sized models with much fewer iterations and function evaluations to convergence. It might be interesting to investigate ways of enhancing this simpler model by adding material parameters that account for anisotropy.

The differences in the tissue behaviour across the three walls were further investigated by examining the variabilities in the c-values of the Fung and Choi-Vitto models in Figure 8. The three walls show that the variabilities for both models increase in the order LV, STW, and RV. The results in this paper were also observed by the authors in a previous experimental study.

Tables 2 – 7 show the material constants in different heart rat regions (i.e LV, RV and STW) for Fung (Table 2), Choi-Vito (Table 3), Polynomial (Anisotropic) (Table 4), Holzapfel (2000) (Table 5), and Holzapfel (2005) (Table 6) hyperelastic models. The average material constants of each hyperelatic models are shown as average and standard deviation across all three heart walls. Appendix A section shows the coefficient materials Fung, Choi-Vito, Polynomial (anisotropic), Holzapfel (2000), Holzapfel (2005) and Four-Fibre-Family hyperelastic models in the left ventricle (LV), septal wall (STW) and right ventricle (RV) for all the samples that are tested in this study.

While the R^2 is a relative measure of how well the model fits dependent variable, a metric called the evaluation index (EI) is any metric that measures the goodness of fit. One such measure may be a metric such as the mean square error (MSE) or its inverse. In this study, its inverse has been used and was calculated by

To magnify the difference between coefficient of determination (R^2) values, the evaluation index (EI) that can assess which models are better than the others was defined [13].

$$Evaluation\ Index\ (EI) = \left[\frac{r - r_{minimum}}{r_{maximum} - r_{minimum}}\right] \quad (2)$$

Where $r = abs[\log_{10}(1 - R^2)]$

EI gives an absolute measure of how much the predicted value is close to the actual value. It gives one a real number to compare against other model results and help one to select the best regression model. In Figure 5, similar trends as the correlation coefficients were observed in the EI's plotted. Notice that the EI's are exactly similar for LV and STW tissues while the RV tissues yield different EI's.

Figure 5 shows the average EI's taken over all the fourteen tests for each of the models under study. The results show that the Polynomial (Anisotropic) model outperforms the other five models in all myocardial tissues with EI's above 90 % goodness of fit. The four-fiber-family and the two Holzapfel models perform equally in the LV and STW myocardial tissue between 50 and 70 % goodness of fit. The Fung and Choi-Vito models yielded very poor goodness of fit in the LV and STW myocardial tissues. In the RV tissues, the Holzapfel models yielded the poorest results, and the Choi-Vito showed better performance than the Four-Fiber-family model.

Figure 6 shows the distribution of the model predicted values for the fourteen tests in the form of the box and whisker plots. Only the Fung and Choi-Vito models show huge spread in the predicted values for the LV and STW myocardial tissues. The other models show remarkably narrow and uniform distribution for these myocardial tissues with lower and upper quartiles lying within 5% range. The predicted value distributions for the Fung and Choi-Vito are wide and rather skewed with lower and upper quartiles covering over 10 % ranges. For the RV myocardial tissue, all models show substantial amounts of skewness in distribution and wider ranges between the lower and upper quartiles. The skewness and

wider spreads in the predicted data for the RV myocardium indicates the relative difficult with which the behaviour of the tissue may be predicted. Additionally, Figure 7 shows the Comparison of c vale for Fung hyperplastic model across three rat myocardia. For Fung model, the distribution of c values across three different wall regions (i.e LV, RV and STW) is stable. Furthermore, c value for Choi-Vito model for septal wall (STW) was shown to be higher that the c value for LV and RV (See Figure 8). This observation is similar to the observation made in the Fung model as shown in Figure 7.

In this paper, the differences in the rat heart myocardium across different walls are investigated by observing the differences in the six different models and their prediction capabilities. This was carried out by examining what model parameters make the Polynomial (Anisotropy) model outperform the other five models; what are the common features between the LV and STW myocardial tissues that make the Polynomial model, Four-Fiber-family, and the two Holzapfel models approximate their behaviour better than the other models; and what unique parameters are there in the Polynomial model that enables it to model RV tissue behaviour the best.

A closer examination of the parameters of the six models shows that the Polynomial, Four-fiber-family and two Holzapfel models share one feature in that they based on the strain invariant approach. As it can be noted from Section 2, this is irrespective of their formalisms whether they are fully polynomial or exponentially implemented. It would therefore imply that to some extent this common feature contributes towards their superiority when modelling LV and STW tissue behaviour. The Fung and Choi-Vito models used in this study have architectures that are based on the Green-Lagrange tensor components, which implement anisotropy exclusively as material orthotropy.

In addition to the above observation, the Polynomial and Four-fiber-family models incorporate contributions of both isotropic strain invariants and transversely isotropic strain invariants. It is observed that these two models have cross-directional material parameters in their architectures. The implementations of the anisotropy in the two models are different as can be observed from Table 1 in Section 2 with the Polynomial model incorporating one more transversely isotropic strain invariant (I_6). Though the differences do not yield much significantly different results for the LV and STW myocardia, there are significant differences for the RV myocardial tissues. It is also important to note that the Polynomial model has four more material parameters than the four-fiber family model. This might imply that the degree of anisotropy in the RV might be much more complex than that in the LV and STW tissues. Hence the prediction of its mechanical behaviour can be best achieved by models that sufficiently represent anisotropy.

However, it is equally important to discuss the computational efficiencies of the models under investigation. In this study it is remarkable how a three-parameter Holzapfel (2005) model closely matched an seven-parameter four-fiber-family and a eleven-parameter polynomial models in predicting the behaviour of the LV and STW tissues. In terms of computational efficiency, this model clearly outperforms the other two big-sized models with much fewer iterations and function evaluations to convergence. It might be interesting to investigate ways of enhancing this simpler model by adding material parameters that account for sufficient modelling of anisotropy as well as adding a polynomial isotropic part.

The differences in the tissue behaviour across the three walls were further investigated by examining the variabilities in the c-values of the Fung and Choi-Vito models in Figure 9. The three walls show that the variabilities for both models increase in the

order LV, STW, and RV. The results in this paper were also observed by the authors in a previous experimental study.

Limitation of the studies

The rat heart conditions and age of all the animals during this study were not known and should have influence the conclusion of the study. Also, the fiber direction of the myocardia was not studies using imaging techniques.

5 Discussion

Six constitutive models were applied to biaxial tensile results obtained from the three different myocardial walls of the rat heart. Fourteen (14) specimen for each myocardial wall were tested. The results show that the polynomial model outperforms the other five models. However, this polynomial model is twelve-parameter model which incorporates both the fiber-orientation and anisotropy effects. It was found that the performance of this model was closely matched by the Holzapfel and Four-fiber family models. It is quite remarkable that the Holzapfel with only five parameters was able to match the performance of the polynomial model on the LV and STW tissue. Thus, the Holzapfel has much more computational benefits than the other models.

The RV myocardial tissue behaviour is the hardest to predict apparently due to its higher degree of anisotropy. Although the polynomial model yields around 90 % correlation, it was observed that this was relatively lower than its correlation on the LV and STW tissue behaviour. There was also largest variability in the EI's c-values for the RV tissues as compared to the LV and STW. At this stage, it therefore seems that anisotropy is the one of the contributing factors to the difficulties in predicting RV tissue behaviour. There might be other factors which require further investigation.

Finally, the poor performance of the Fung and Choi-Vito models is further evidence to the fact that myocardial tissue behaviour cannot be accurately represented by models that do not incorporate fiber orientation and anisotropy. Notice that all models that yield better performance have at least one of the two factors. On the other hand, the Fung and Choi-Vitto models have neither of these factors. Despite the large number of material parameters in the Fung model, it still yielded poor results.

6 Conclusion

We successfully employed the biaxial mechanical data to demonstrate the relationship between the mechanical l behaviour of various regions in the rat heart. The established anisotropic materials properties could be utilised in the understanding of various disease mechanisms by using the rat model. Inverse finite element model and genetic algorithm were employed to identify the parameters of Fung orthotropic hyperelastic strain energy function in three regions (RV, LV and STW) in the rat heart. The identified material parameters will provide new platform for FE investigations of mechanical aspects of various therapies when using rat models.

Acknowledgements

This study was supported financially by the University of South Africa. Any opinion, findings and conclusions or recommendations expressed in this publication are those of the authors and therefore the University of South Africa does not accept any liability in regard thereto.

Conflict of Interests

Conflicts of interest do not exist.

Author contributions

F.N, H.N, T.F, N.D and T.P contributed to conception, design, data acquisition, analysis, and interpretation, drafted the manuscript, H.N, T.P and F.N contributed to the interpretation of the data and critically revised the manuscript, and finally F.N, H.N, T.F, N.D and T.P contributed to conception, design, data analysis, and interpretation, drafted and critically revised the manuscript. All authors gave final approval and agree to be accountable for all aspects of the work.

Funding

This research received no specific grant from any funding agency in the public, commercial, or not-for-profit sectors.

Corresponding author

Correspondence to Fulufhelo Nemavhola

Declarations Ethics approval and consent to participate

The animal study ethics was approved by the Faculty of Health Sciences Animal Ethics Committee of the University of Cape Town on 6th of May 2019 under reference number FHS AEC REF 019-019

Consent for publication

Not applicable.

Competing interests

The authors declare that they have no competing interests.

References

1. Murphy, E. and B. Shelley, *The right ventricle—structural and functional importance for anaesthesia and intensive care.* BJA Education, 2018. **18**(8): p. 239-245.
2. Ngwangwa, H.M., T. Pandelani, and F. Nemavhola, *The Application of Standard Nonlinear Solid Material Models in Modelling the Tensile Behaviour of the Supraspinatus Tendon.* Preprints, 2021. **2021080298**.
3. Ngwangwa, H.M. and F. Nemavhola, *Evaluating computational performances of hyperelastic models on supraspinatus tendon uniaxial tensile test data.* Journal of Computational Applied Mechanics, 2021. **52**(1): p. 27-43.

4. Nemavhola, F., *Biaxial quantification of passive porcine myocardium elastic properties by region.* Engineering Solid Mechanics, 2017. **5**(3): p. 155-166.
5. Nemavhola, F., *Study of biaxial mechanical properties of the passive pig heart: material characterisation and categorisation of regional differences.* International Journal of Mechanical and Materials Engineering, 2021. **16**(1): p. 1-14.
6. Guccione, J.M., K.D. Costa, and A.D. McCulloch, *Finite element stress analysis of left ventricular mechanics in the beating dog heart.* Journal of biomechanics, 1995. **28**(10): p. 1167-1177.
7. Masithulela, F.J., *Computational biomechanics in the remodelling rat heart post myocardial infarction.* 2016.
8. Masithulela, F., *Bi-ventricular finite element model of right ventricle overload in the healthy rat heart.* Bio-medical materials and engineering, 2016. **27**(5): p. 507-525.
9. Masithulela, F. *The effect of over-loaded right ventricle during passive filling in rat heart: A biventricular finite element model*. in *ASME International Mechanical Engineering Congress and Exposition*. 2015. American Society of Mechanical Engineers.
10. Masithulela, F. *Analysis of passive filling with fibrotic myocardial infarction*. in *ASME international mechanical engineering congress and exposition*. 2015. American Society of Mechanical Engineers.
11. Masithulela, F. *The Effect of Over-Loaded Right Ventricle During Passive Filling in Rat Heart: A Biventricular Finite Element Model*. in *ASME 2015 International Mechanical Engineering Congress and Exposition*. 2015.
12. Nemavhola, F., *Detailed structural assessment of healthy interventricular septum in the presence of remodeling infarct in the free wall–A finite element model.* Heliyon, 2019. **5**(6): p. e01841.
13. Nemavhola, F., *Fibrotic infarction on the LV free wall may alter the mechanics of healthy septal wall during passive filling.* Bio-medical materials and engineering, 2017. **28**(6): p. 579-599.
14. Nemavhola, F., *Mechanics of the septal wall may be affected by the presence of fibrotic infarct in the free wall at end-systole.* International Journal of Medical Engineering and Informatics, 2019. **11**(3): p. 205-225.
15. Yin, Z., et al., *Cardiac wall mechanics analysis in hypertension-induced heart failure rats with preserved ejection fraction.* Journal of Biomechanics, 2020. **98**: p. 109428.
16. Sirry, M.S., et al., *Characterisation of the mechanical properties of infarcted myocardium in the rat under biaxial tension and uniaxial compression.* journal of the mechanical behavior of biomedical materials, 2016. **63**: p. 252-264.
17. Chuong, C. and Y. Fung, *Three-dimensional stress distribution in arteries.* Journal of biomechanical engineering, 1983. **105**(3): p. 268-274.
18. Choi, H.S. and R. Vito, *Two-dimensional stress-strain relationship for canine pericardium.* Journal of biomechanical engineering, 1990. **112**(2): p. 153-159.
19. Holzapfel, G.A., T.C. Gasser, and R.W. Ogden, *A new constitutive framework for arterial wall mechanics and a comparative study of material models.* Journal of elasticity and the physical science of solids, 2000. **61**(1): p. 1-48.
20. Holzapfel, G.A., et al., *Determination of layer-specific mechanical properties of human coronary arteries with nonatherosclerotic intimal thickening and related constitutive modeling.* American Journal of Physiology-Heart and Circulatory Physiology, 2005. **289**(5): p. H2048-H2058.
21. Ferruzzi, J., D.A. Vorp, and J. Humphrey, *On constitutive descriptors of the biaxial mechanical behaviour of human abdominal aorta and aneurysms.* Journal of the Royal Society Interface, 2011. **8**(56): p. 435-450.

22. Baek, S., et al., *Theory of small on large: potential utility in computations of fluid–solid interactions in arteries.* Computer methods in applied mechanics and engineering, 2007. **196**(31-32): p. 3070-3078.
23. Bursa, J., et al. *Implementation of hyperelastic models for soft tissues in FE program and identification of their parameters*. in *Proceedings of the Sixth IASTED International Conference on Biomedical Engineering*. 2008.
24. Javani, S., M. Gordon, and A.N. Azadani, *Biomechanical properties and microstructure of heart chambers: A paired comparison study in an ovine model.* Annals of biomedical engineering, 2016. **44**(11): p. 3266-3283.
25. Humphrey, J., R. Strumpf, and F. Yin, *Biaxial mechanical behavior of excised ventricular epicardium.* American Journal of Physiology-Heart and Circulatory Physiology, 1990. **259**(1): p. H101-H108.
26. Fatemifar, F., et al., *Comparison of biomechanical properties and microstructure of trabeculae carneae, papillary muscles, and myocardium in the human heart.* Journal of biomechanical engineering, 2019. **141**(2).
27. Ghaemi, H., K. Behdinan, and A. Spence, *In vitro technique in estimation of passive mechanical properties of bovine heart: Part I. Experimental techniques and data.* Medical engineering & physics, 2009. **31**(1): p. 76-82.
28. Sommer, G., et al., *Biomechanical properties and microstructure of human ventricular myocardium.* Acta biomaterialia, 2015. **24**: p. 172-192.
29. Ateshian, G.A. and K.D. Costa, *A frame-invariant formulation of Fung elasticity.* Journal of biomechanics, 2009. **42**(6): p. 781-785.
30. Chagnon, G., M. Rebouah, and D. Favier, *Hyperelastic energy densities for soft biological tissues: a review.* Journal of Elasticity, 2015. **120**(2): p. 129-160.
31. Nemavhola, F., et al., *Passive Biaxial Tensile Dataset of Three Main Rat Heart Myocardia: Left Ventricle, Mid-Wall and Right Ventricle.* Preprints, 2021. **2021080153**(Version 1).
32. Ngwangwa, H., et al., *Determination of Cross-directional and Cross-Wall Variations of Passive Biaxial Mechanical Properties of Rat Myocardium.* Preprints, 2021. **2021090244**.
33. Anssari-Benam, A., et al., *Rate-dependency of the mechanical behaviour of semilunar heart valves under biaxial deformation.* Acta biomaterialia, 2019. **88**: p. 120-130.
34. van Disseldorp, E.M., et al., *Reproducibility assessment of ultrasound-based aortic stiffness quantification and verification using Bi-axial tensile testing.* Journal of the mechanical behavior of biomedical materials, 2020. **103**: p. 103571.
35. D'Amore, A., et al., *Bi-layered polyurethane–extracellular matrix cardiac patch improves ischemic ventricular wall remodeling in a rat model.* Biomaterials, 2016. **107**: p. 1-14.
36. Caulk, A.W., et al., *Quantification of the passive and active biaxial mechanical behaviour and microstructural organization of rat thoracic ducts.* Journal of The Royal Society Interface, 2015. **12**(108): p. 20150280.
37. Robertson, D. and D. Cook, *Unrealistic statistics: how average constitutive coefficients can produce non-physical results.* Journal of the mechanical behavior of biomedical materials, 2014. **40**: p. 234-239.
38. Wang, Z., M.J. Golob, and N.C. Chesler, *Viscoelastic properties of cardiovascular tissues.* Viscoelastic and viscoplastic materials, 2016. **2**: p. 64.
39. Granzier, H.L. and S. Labeit, *The giant protein titin: a major player in myocardial mechanics, signaling, and disease.* Circulation research, 2004. **94**(3): p. 284-295.
40. Helmes, M., et al., *Mechanically driven contour-length adjustment in rat cardiac titin's unique N2B sequence: titin is an adjustable spring.* Circulation research, 1999. **84**(11): p. 1339-1352.
41. Grignola, J.C., et al., *Improved right ventricular–vascular coupling during active pulmonary hypertension.* International journal of cardiology, 2007. **115**(2): p. 171-182.

42. Bellofiore, A. and N.C. Chesler, *Methods for measuring right ventricular function and hemodynamic coupling with the pulmonary vasculature.* Annals of biomedical engineering, 2013. **41**(7): p. 1384-1398.
43. Sacks, M. and C. Chuong, *Biaxial mechanical properties of passive right ventricular free wall myocardium.* 1993.

Figures

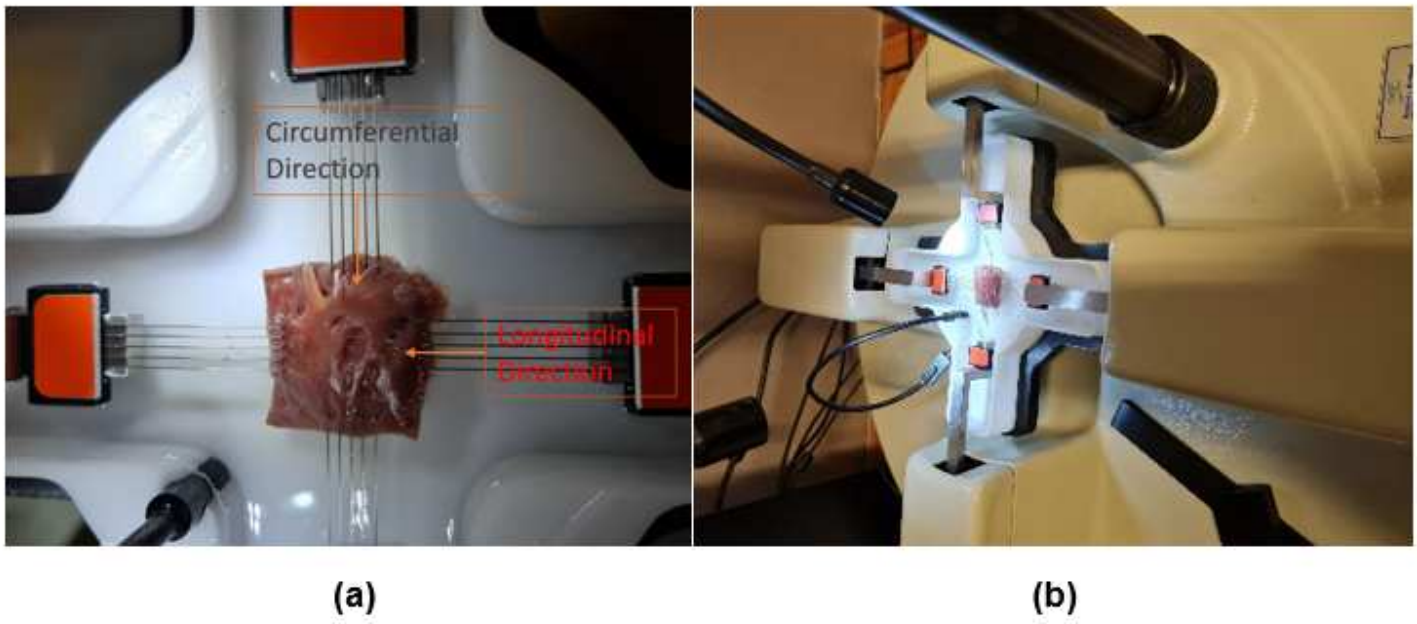

Figure 1

(a) Sample attached on the (BioTester 5000 CellScale, Waterloo, Canada) showing both longitudinal and circumferential direction (b) Experimental set up of equi-biaxial mechanical testing of sheep heart looking at different regions in Left ventricle (LV), septal wall (SPW) and Right ventricle (RV)

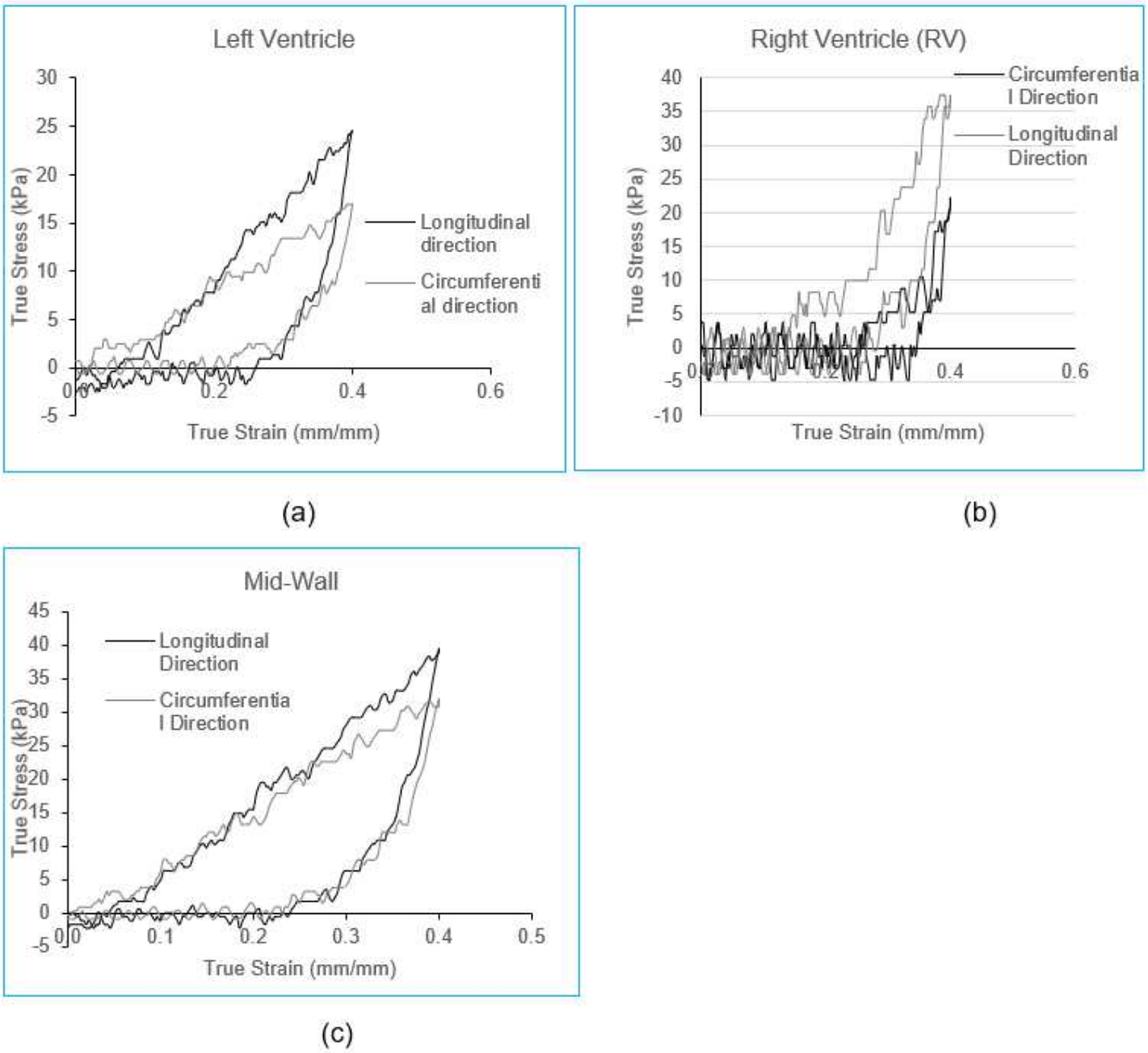

Figure 2

True stress and strain curve of the sample LV of (a) LV, (b) RV and (c) Mid-wall (Septal wall)

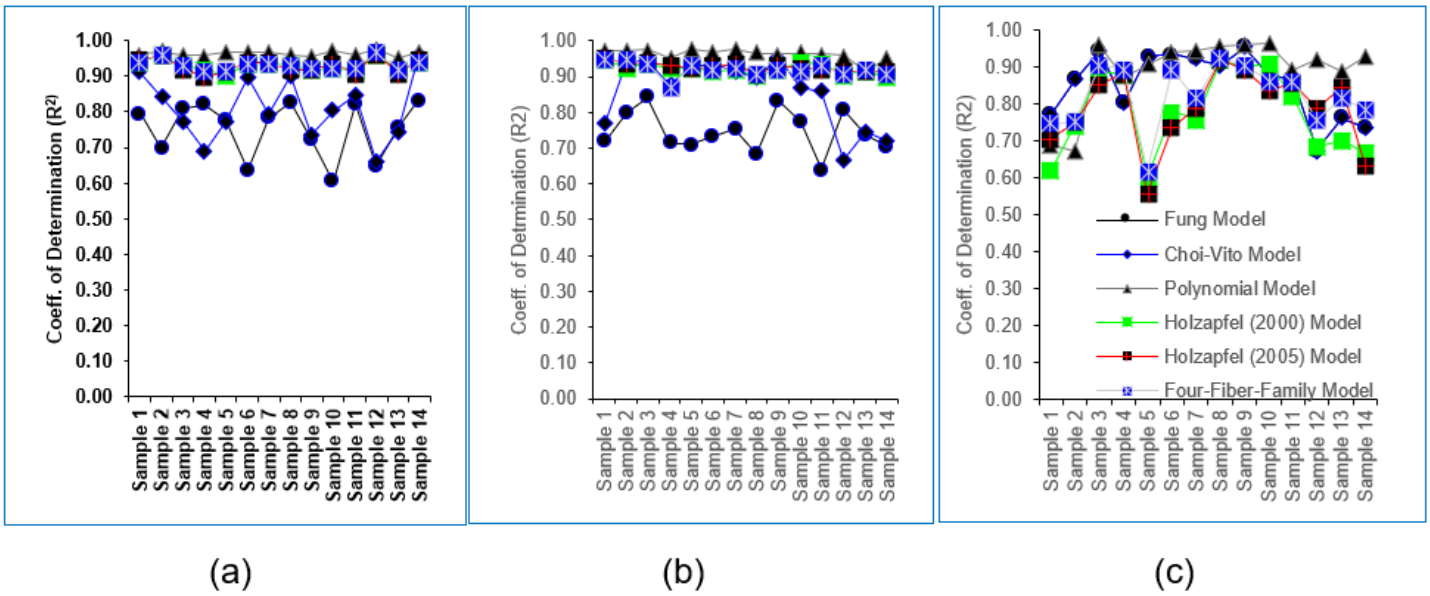

Figure 3

Coefficient of determination (R2) plotted again all samples comparing fitting of Fung, Choi-Vito, Polynomial (anisotropic), Holzapfel (2000), Holzapfel (2005) and Four-Fibre-Family hyyperelastic models in the (a) LV, (b) STW and (c) RV.

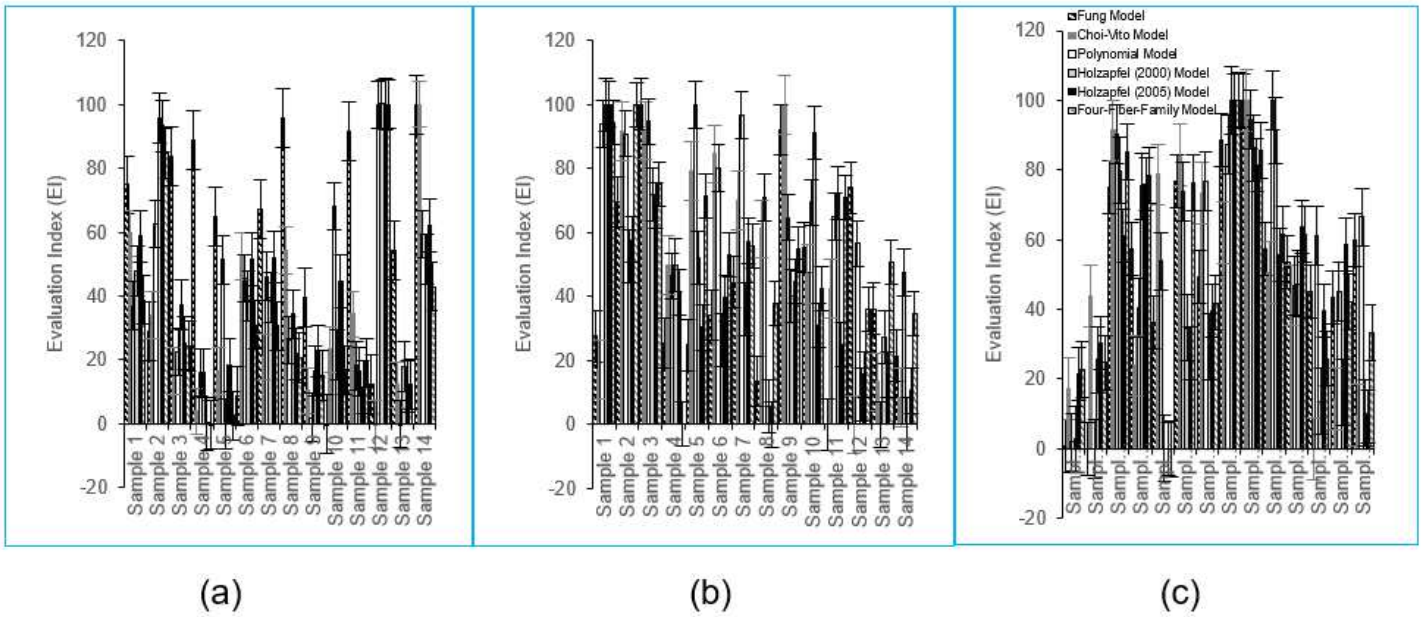

Figure 4

Evaluation Index (EI) plotted with standard error of fitted Fung, Choi-Vito, Polynomial (anisotropic), Holzapfel (2000), Holzapfel (2005) and Four-Fibre-Family hyperelastic models in the (a) LV, (b) STW and (c) RV.

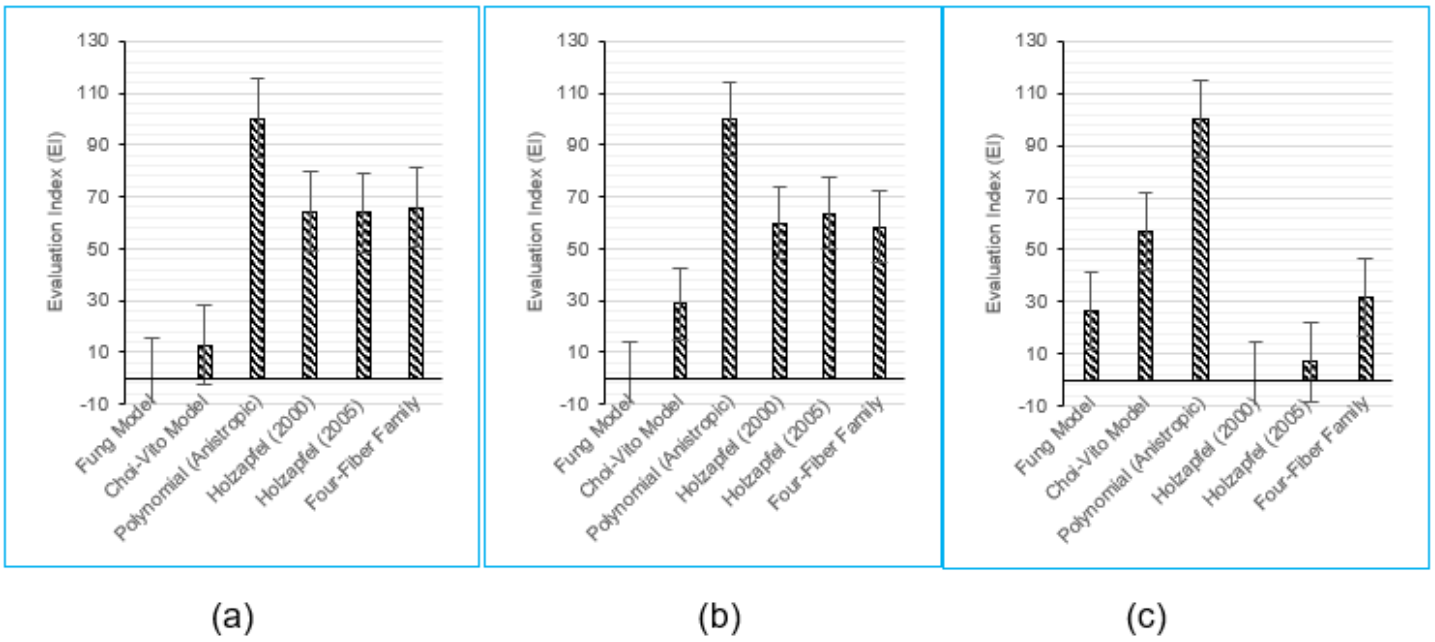

Figure 5

Average Evaluation Index (EI) plotted with standard error of fitted Fung, Choi-Vito, Polynomial (anisotropic), Holzapfel (2000), Holzapfel (2005) and Four-Fibre-Family hyperelastic models in the (a) LV, (b) STW and (c) RV.

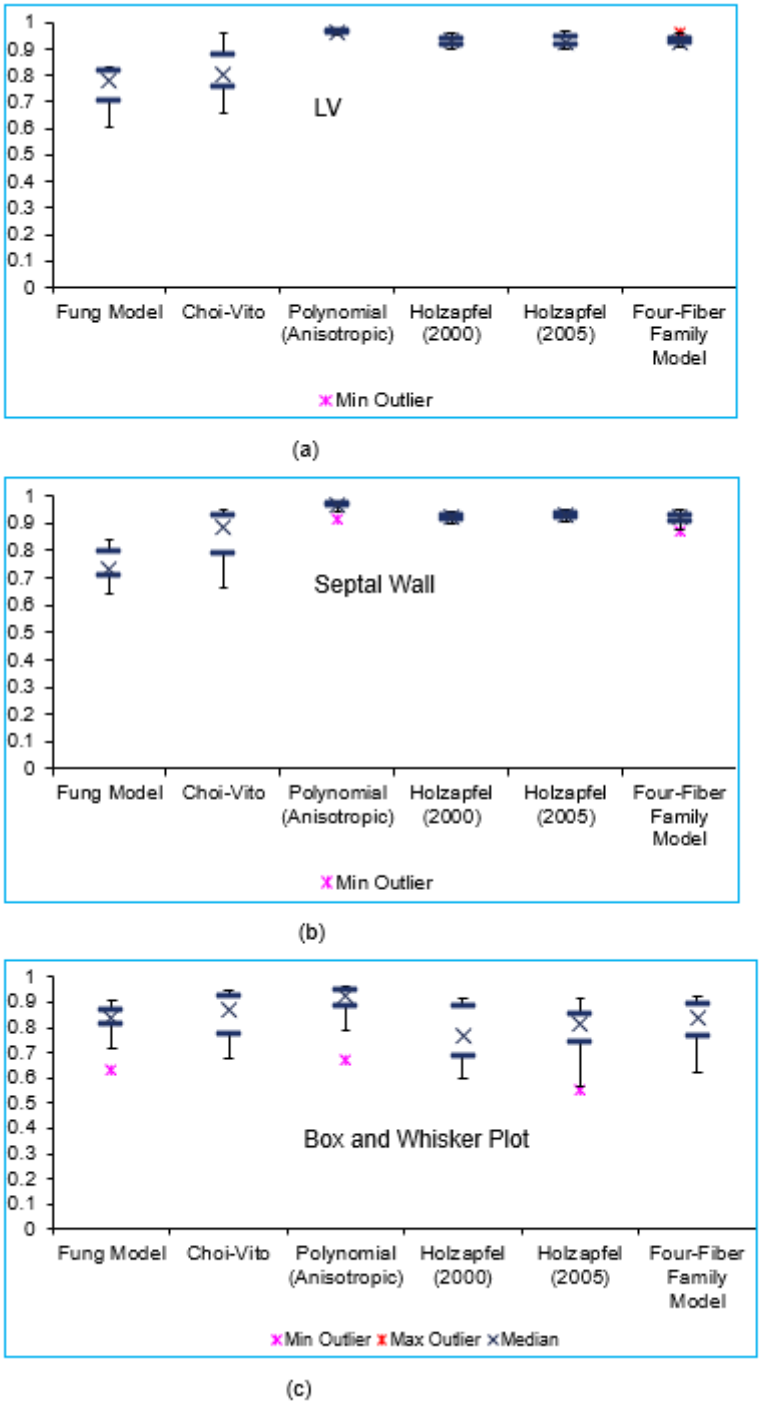

Figure 6

Boxplot of the Coefficient of Determination (R2) of fitted Fung, Choi-Vito, Polynomial (anisotropic), Holzapfel (2000), Holzapfel (2005) and Four-Fibre-Family hyperelastic models in the (a) LV, (b) STW and (c) RV.

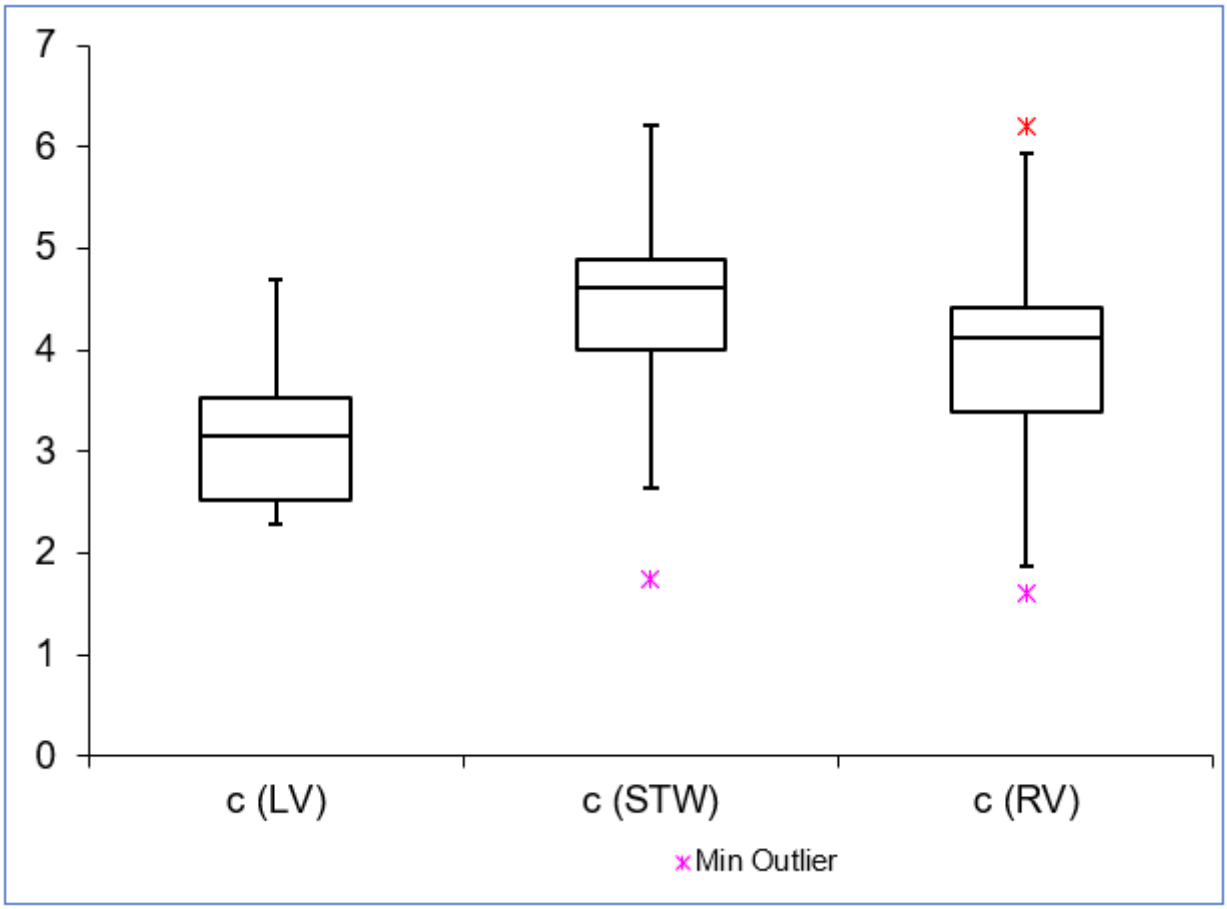

Figure 7

Comparison of c vale for Fung hyperplastic model across three rat myocardia (i.e left ventricular, septal wall and right ventricle)

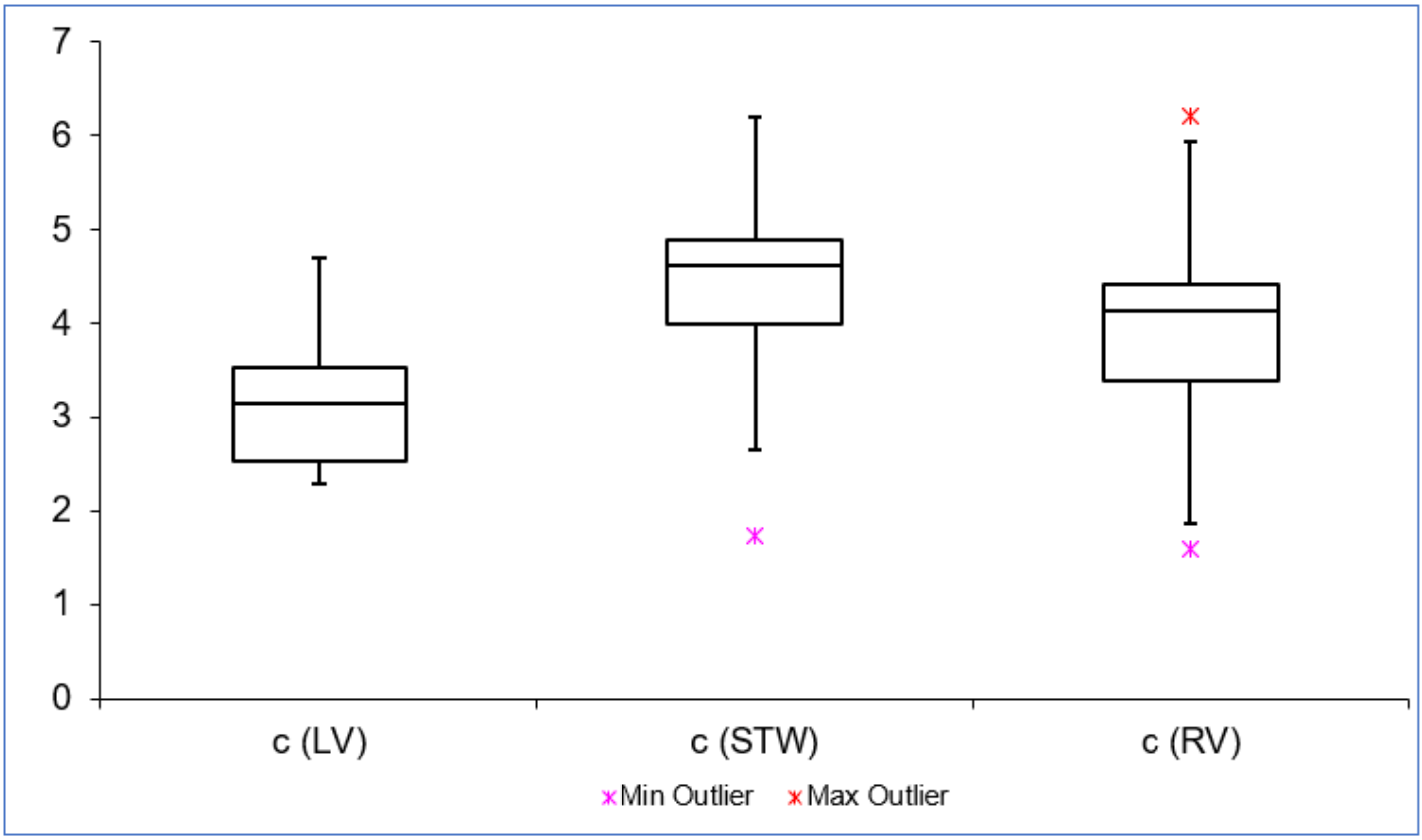

Figure 8

Comparison of c vale for Choi-Vito hyperplastic model across three rat myocardia (i.e left ventricular, septal wall and right ventricle)

Supplementary Files

This is a list of supplementary files associated with this preprint. Click to download.

- Paper77Tables001.docx